

Analysis of a novel vertical axis twin-rotor wind turbine performance in an urban environment

Shivangi SACHAR¹ , Piotr DOERFFER¹, Pawel FLASZYNSKI¹, Krzysztof DOERFFER²,
Joanna GRZELAK², and Andrzej REITER³

¹ Institute of Fluid-Flow Machinery, Polish Academy of Sciences, Gdańsk, Poland

² Faculty of Mechanical Engineering and Ship Technology, Gdańsk University of Technology, Gdańsk, Poland

³ Electronic Services Company, Gdańsk, Poland

Abstract. The study presented in this paper demonstrates the findings concerning a twin-rotor vertical-axis wind turbine patented by IMP PAN. Motivation for this wind turbine design was significantly driven by the need to exploit the wind energy available in an urban environment. The primary anticipated advantage is the substitution of the Savonius rotor by a new system allowing lighter and cheaper construction. The improvement of the wind turbine prototype presented took over three years, and the final modified version of the wind turbine underwent long-term testing. The paper presents a detailed description of the operational parameters and measured characteristics. One of the main objectives of the research was to test this novel wind turbine in a real environment, which is highly influenced by incoming wind conditions. The wind characteristics experienced by the turbine mounted on the roof of the IMP PAN building during the test period were demonstrated using Weibull distributions. Apart from wind conditions, the main goal of the measurements was to estimate the power characteristics of the novel wind turbine design. Measurements included output of the generator, consisting of voltage and current, the product of which allowed for determining the power extracted from the generator. Another important quantity was the speed of rotation of both turbines. The ratio of wind speed and the speed of rotation allowed for estimating the quality of the power extraction algorithm, which should be operated at $TSR \approx 1.0$. The results obtained show that the power extraction algorithm could still be improved. The paper also contains an analysis of the dynamic effect of wind fluctuation on the rotor behavior, and the determination of the correlation of rotor response delay to wind gusts. The reduction of the wind velocity peak effect on energy production is discussed.

Keywords: wind energy; vertical axis wind turbine; Savonius rotor; twin-rotor wind turbine.

1. INTRODUCTION

With an increasing population in urban areas, a great demand for power generation is predicted. Such an environment would benefit greatly from the potential abundant use of safe, quiet, and renewable energy resources [1, 2]. Numerous studies around wind energy have been conducted over the past decades. Technological advancements and the availability of wind energy in such locations attract various researchers to wind turbines [3, 4], which are often considered as an element of hybrid systems together with photovoltaic [5, 6]. Reasons for this interest can be attributed to the reduction in the energy transportation distance, increase in the power source availability, efficiency of energy, and reduction in transmission losses [7]. The complex structures of buildings and their layout affect the wind patterns around them. Additional effects are observed when the spacing between buildings is lower compared to their heights. This leads to an increase in the wind velocity in such gaps, strongly dependent on the wind direction [8, 9].

Horizontal axis wind turbines are highly effective for wind energy conversion, but they have not proven to contribute to low-cost energy conversion of these turbines. Compared to their horizontal counterparts in such conditions, small vertical axis wind turbines (VAWTs) operate better [10]. Small wind turbines are preferable when it comes to their integration with buildings due to the presence of complex flows [7, 9, 11], and their advantages include ease of installation and integration to the grid [12]. Moreover, they cause no harm to migrating birds, people, and the urban infrastructure [13, 14].

Other attractive features of VAWTs are the ability to start at low winds and ease of maintenance [15]. These key features inspired a lot of research aiming at the enhancement of their effectiveness [16–20]. This effect has also been achieved by blade shape modifications and optimization [21, 22], introducing blade twist. In addition, small wind turbines of the Savonius type do not overspin at high winds, which protects the rotor against damage and overspinning. This is a crucial factor when working in an urban environment, due to the presence of changeable wind patterns and turbulence intensities.

The benefits of installing small VAWTs in an urban environment motivated the development of a twin rotor turbine at IMP PAN [7]. This innovative prototype was mounted on the roof of the research center, and its configuration, together with mea-

*e-mail: shivangi_sachar@hotmail.com

Manuscript submitted 2025-04-16, revised 2025-07-04, initially accepted for publication 2025-07-10, published in November 2025.

surement data, is discussed in detail in the following sections. The illustration of its location is presented in Fig. 1. The objective of this paper is to demonstrate the results of this turbine operation performance in a natural wind condition.



Fig. 1. Innovative WT prototype on the roof of IMP PAN building

2. VERTICAL AXIS TURBINE AND TWIN ROTOR CONCEPT

In the twin-rotor wind turbine, a single large Savonius rotor (Fig. 2a) is substituted with a combination of two vertical rotor lines at the tips of a central guiding plate (Fig. 2b). The use of much smaller rotors leads to a reduction of wind turbine costs. The innovative system delivers similar power as the large Savonius rotor [7], while maintaining the safety features of drag-

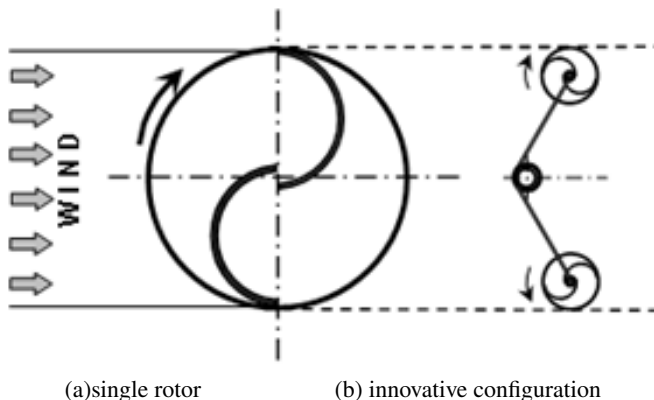


Fig. 2. Savonius rotor and innovative twin rotor turbine [6]

driven turbines. The wind stream is 1.2 m wide while the rotor diameter is 0.25 m.

The guiding plate between the small rotors stops the incoming wind. It causes the build-up of dynamic pressure from the wind on the upwind side of the turbine. This increased pressure causes wind to accelerate over the guiding plate tips, where the air reaches a higher velocity than the incoming wind speed. In this place, small rotors are implemented. Due to increased wind speed around the small rotors, the power generated by these two rotors is equivalent to the power produced by the large Savonius rotor.

The prototype of the twin-rotor wind turbine [7] (Fig. 1) contains several features, which were validated during a long testing period described in the present paper. These were:

- Effectiveness of power generation
- Speed of rotation
- Power extraction algorithms

A critical issue during the implementation of the prototype described here was the influence of the rotor configuration. The effect of the rotor segmentation was investigated and presented in [23]. The segmentation of Savonius rotors is a recognized topic in the literature. Most typically, the height of a segment (H) is equal to one or two rotor diameters (D), of aspect ratio $AR = H/D = 1$ or 2 . There is not much information on the effect of this rotor aspect, as it requires experiments [24–26] or fully three-dimensional unsteady numerical simulations [27–29]. Careful numerical analysis in [28] indicates that the rotor effectiveness increases with segment elongation, which was studied up to the aspect ratio of $AR = 5$. It is also suggested by the author of [28] that rotor elongation should not be smaller than $AR = 2$. The information available in the literature on the segmented rotors is sometimes contradictory. The material found in the literature does not allow unequivocal conclusions.

Therefore, a more significant difference in the number of segments was used in [23]. Single-segment and four-segment rotors were investigated, and it was observed that the difference in aerodynamic characteristics depended on the wind speed. A small range of wind speeds was investigated in the paper, which proved to be essential, demonstrating the difference in effectiveness caused by rotor segmentation [23].

In Fig. 3, the maximum effectiveness C_P is plotted against wind velocity. The plot shows higher effectiveness of the single-segment rotor in the entire range of the considered wind velocities. The difference between the rotors becomes crucial at low wind velocities, whereas at higher velocities, the difference is of lesser importance.

The power coefficient is expressed by

$$C_P = \frac{P}{P_0}, \quad (1)$$

where

$$P_0 = \frac{\rho}{2} V_W^3 \quad \text{maximum available wind power}, \quad (2)$$

where P – power measured on the generator, A – rotor projection area, ρ – air density, V_W – wind speed.

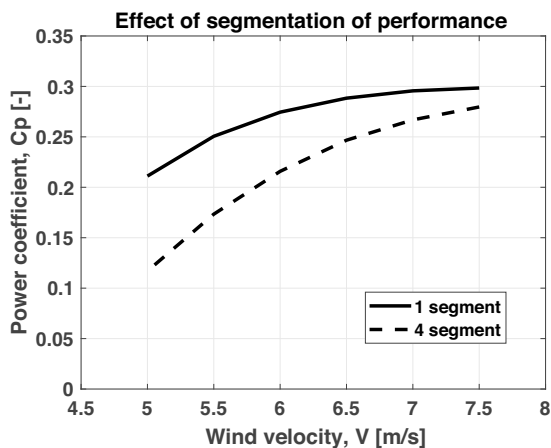


Fig. 3. Effectiveness (C_p) for 1-segment and 4-segment rotors [23]

The observation in Fig. 3 is important from the application point of view, indicating that at low wind speed conditions, it is advisable to use single-segment rotors. The explanation of the development of the flow structures responsible for this effect is still a challenge and calls for extremely advanced time-resolved measurements and high-fidelity unsteady numerical simulations.

Both 4-segment and 1-segment rotors were used on the prototype turbine, as shown in Fig. 4. After three years of operation, these rotors withstood the operational conditions. Assessment of the innovative rotor and the whole turbine presented here is highly challenging. The unsteadiness of wind in an urban environment creates considerable difficulties. In general, open-air real conditions of wind turbine testing never confirms the power data provided by the wind turbine manufacturers [13, 30].



Fig. 4. Prototype turbine

3. METHODOLOGY OF WIND CONDITIONS DESCRIPTION

Testing of a wind turbine in real conditions is a challenging task. First, the wind is significantly fluctuating, and a more detailed statistical representation of wind over a certain period

is necessary to provide detailed information about the wind conditions in which the wind turbine is tested. In this paper, a typical representation of wind by the Weibull distribution is used. Weibull coefficients are determined to allow the reader to compare the operational conditions with test cases of other authors.

A Weibull parameter study is included in this paper, consisting of the shape factor k and the scale factor c . The shape factor signifies the range (width) of the wind speed distribution. A typical range of k is 1.5–2.5. A value less than 2 suggests weak winds, and a value of 2 demonstrates an equal amount of strong and weak winds. Thus, k with a value of $k = 2$ or more is preferable when selecting the location for the wind turbine operation. On the other hand, the scale factor c gives an idea about the mean wind speed. The higher the value, the greater the mean wind speed. These Weibull coefficients can be calculated in a number of ways.

The literature on the determination of Weibull coefficients is extremely broad, but some information should be provided here. Wind data collected at different heights from the ground for the ‘AL-Najaf’ site in Iraq are presented in [31]. The test heights taken into consideration were 10 m, 30 m, and 50 m. Six different techniques to calculate the Weibull parameters were studied. The methods, including RMSE, chi-square, correlation coefficient (R), and R^2 , were ranked based on data fitting. It was concluded that no method could be selected as best for all cases. The quality of fit for the results obtained from any of the techniques used depends on the wind data and needs to be evaluated using the data fitting procedures. For the particular study in [33], it was the power density method and maximum likelihood estimation that gave the best fit to the Weibull distribution.

RMSE is the square root of the average total error squared. It is one of the most frequently used methods for performing error analysis to compare the goodness of fit between different techniques being used [33]. An error close to zero is desirable for the above-mentioned errors. The MAPE is the percentage of the absolute error between the observed and predicted data. It is a relatively simple method to predict the error [32]. R^2 analyses the variance of the method by finding a linear relationship between the observed sample data and the predicted data using the Weibull function. The Chi-Square test is a scale-independent method, i.e., it can be used to compare sample data of varying lengths. This test can be used for both independent variables, two data sets, and multiple data sets. It is easy to compute and provides a lot of information about not only the group error but also the independent variables contributing the most to these errors [34].

A comparable study was performed in [35] comparing seven Weibull factor estimation techniques using various statistical tools. The study included three different weather stations, and the measurements were taken at two different heights: 20 m and 30 m. The methods were ranked on the basis of their effectiveness using several statistical tools, namely, the root mean square error, the chi-square error, the R^2 , the mean percentage error, and the relative percentage error.

The method of moments yielded the best-fitting curve for this study [35]. According to this analysis, the method of moments

produced the best results, followed by the maximum likelihood method (MLM) and the power density method (PDM). Some of the other methods in the study included the equivalent energy method (EEM) and the graphical method (GM).

For the present investigation, three methods were considered, namely: the standard deviation method (STDm), the maximum likelihood estimation (MLE), and the method of moments (MOM).

The wind conditions in our test case were investigated with the above background. An example of the results is presented in Figs. 5 and 6. The wind is extremely irregular, especially in the urban environment. A typical example of sampling every second for 1000 samples is shown in Fig. 5. It is clear that a time span of 1000 seconds is incredibly short; however, a longer record would not be readable in such plots.

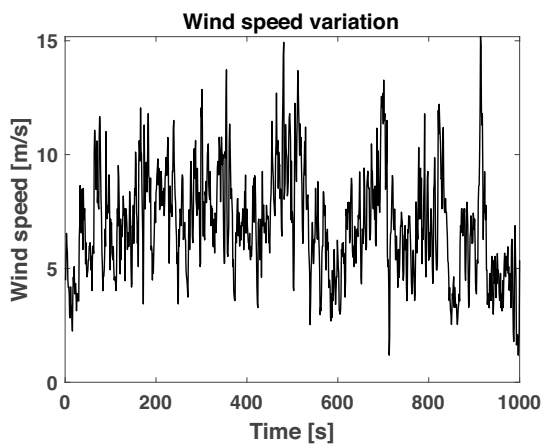


Fig. 5. Wind velocity fluctuations in time

The average velocity for this particular data set in Fig. 5 is $V_{AV} = 6.26$ m/s with the standard deviation of $SD = 2.175$ m/s, which means that there is a 35% fluctuation in the wind speed. This indicates that the wind is of an extremely low velocity and with remarkably high unsteadiness. Unfortunately, these difficult wind conditions are typical of the wind characteristics in urban environments.

As the rotors in the innovative solution are smaller than the large Savonius rotor, it is apparent that the rotational velocity of the small rotors will be higher at the same wind velocity. It may be expected that the maximum power coefficient for an innovative solution should be at the level of $TSR = 1.0$ (as in the Savonius rotor in Fig. 11) or more, where TSR is the ratio of rotor tip velocity to wind velocity. At such rotational speeds, the innovative solution could deliver power equal to one large rotor. Therefore, it is useful to plot the value of the TSR for each measurement point (Fig. 6).

As explained in Section 4 of this paper, the values of the TSR signify how well the control system loads the generators. The control algorithm must cope with the fast wind velocity variation and the rotors response time to the load change. Therefore, the effect of the load control in the wind turbine may be verified by the TSR value. It is expected that the maximum power is extracted at $TSR \geq 1.0$. Therefore, it is useful to analyze in this

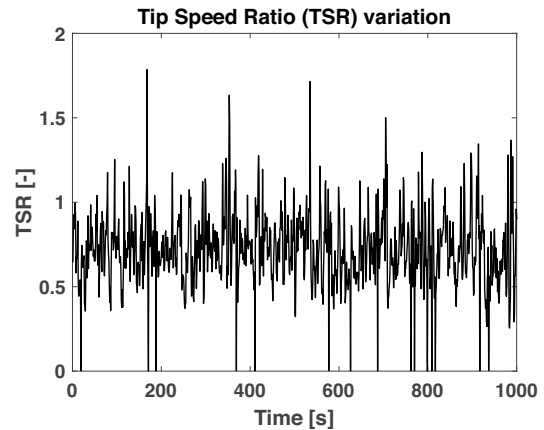


Fig. 6. Values of TSR for samples from Fig. 5

respect the plot in Fig. 6. As the data presented is for 1000 samples only, the conclusions are not general but indicative. The average TSR value in Fig. 6 is around 0.7. This value of the TSR below 1.0 indicates that the wind turbine control systems are not yet adjusted to extract maximum power.

The loading of the rotors is excessive, diminishing the rotation speed. Further improvement of the wind turbine must reduce the load to increase the speed of rotation, which will lead to an increase in power.

The Weibull parameters were calculated using different methods. It is seen that the results present negligible differences. Thus, statistical techniques are used to evaluate the best method. As per the results of the statistical error calculated, MOM is giving the best results, followed by STDm and MLE. Figure 7 demonstrates the Weibull curve according to MOM, where all three curves overlap.

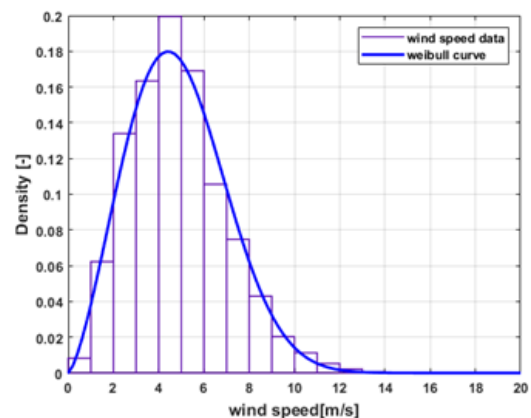


Fig. 7. Weibull plot using different techniques

For the particular day discussed here, the wind characteristics are described by:

- Shape factor $k - 2.44$
- Scale factor $c - 5.48$
- Average wind speed – V_{AV} 5.04 m/s

These wind conditions show low winds at the location of the wind turbine tests. At such velocities, lift-driven turbines, HAWT and VAWT of the Darrieus type, just start to operate.

4. ANALYSIS OF WIND CONDITIONS DURING TESTS

The data set contains one-day measurements that consisted of 65 536 sample points and was taken within 18.2 hours. This data set concerned a relatively small wind flow case.

The example in Fig. 5 concerns a brief time only, which does not have to be representative of the tested measurement period. The whole test discussed in this paper concerns about 18 hours. Taking all this data into consideration, the turbulence intensity was determined. Typically, the turbulence intensity of wind, $TI = SD/V_{AV}$, is determined from the 10-minute averaged values. However, for the short test period analyzed in this paper, this approach provides insufficient data points, and the scope of wind velocities is reduced. Therefore, Fig. 8 shows the turbulence intensity using 1-minute average values. The mean values of wind velocity and TI are similar for these two approaches.

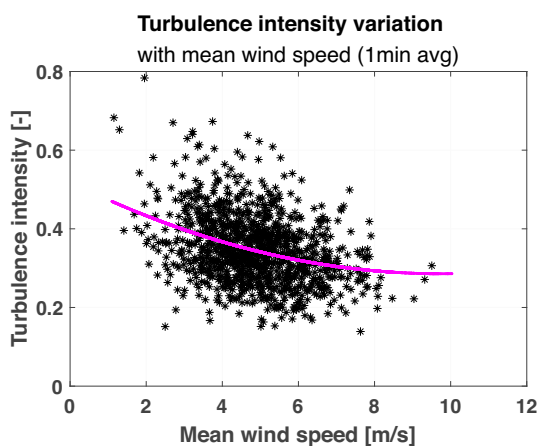


Fig. 8. Turbulence intensity for 1-minute average versus wind mean speed

The values of TI correspond well to the values in paper [13] for cases of wind blowing from land with a high turbulence level. This is not surprising as our wind turbine is installed on the IMP PAN building, surrounded by a heterogeneous terrain of complex structures, trees, open fields and other buildings. The urban environment is connected with a high turbulence level of wind. Typically, the value of TI reduces with wind velocity, as shown in Fig. 8. Therefore, one can conclude that the location of the presented innovative wind turbine corresponds to a typical urban environment with high wind turbulence.

5. INNOVATIVE WIND TURBINE SETUP AND TESTING

Important dimensions of the innovative system are presented in Fig. 9, which is a cross-section through the turbine, shown in Fig. 4.

The total operational height of the wind turbine is $HT = 3$ m. The width of the innovative turbine, including the guiding plate and rotors, is $LT = 1.2$ m (Fig. 9). These give the projection area of the innovative wind turbine $AT = 3.6$ m². Figure 10 presents the expected power generation curves assuming that the wind turbine effectiveness is 10, 15, or 20%. The presented total power is generated by two sets (lines) of rotors. At the nominal

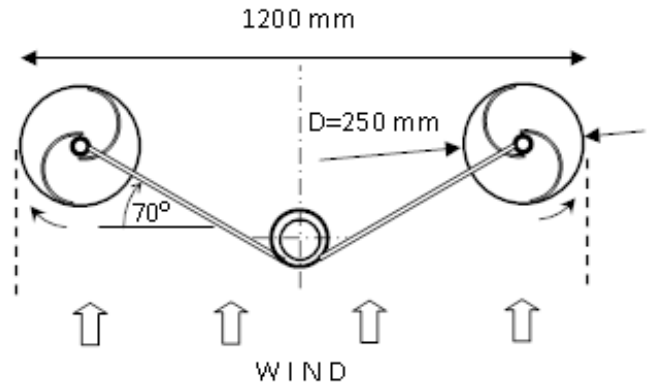


Fig. 9. Test turbine dimensions

wind of 12 m/s and 20% effectiveness, the obtained total power is about 800 W. The generated power depends significantly on the wind turbine effectiveness, as shown in Fig. 10.

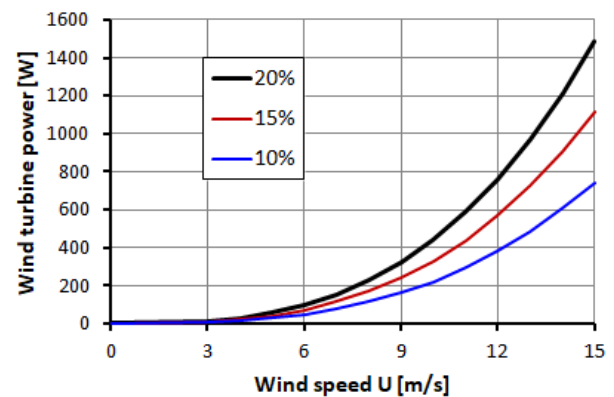


Fig. 10. Power generation for chosen effectiveness and wind speeds

As usual, the curves in Fig. 10 are created by the maximum power for each wind velocity. For the Savonius rotor, it is known that this happens when the speed of the rotor circumference velocity V_T is about 90% of the wind speed V_W , which gives $TSR = V_T/V_W \approx 0.9$ (Fig. 11).

The typical power characteristic of the Savonius rotor is presented in Fig. 11 as a function of $C_p = f(TSR)$.

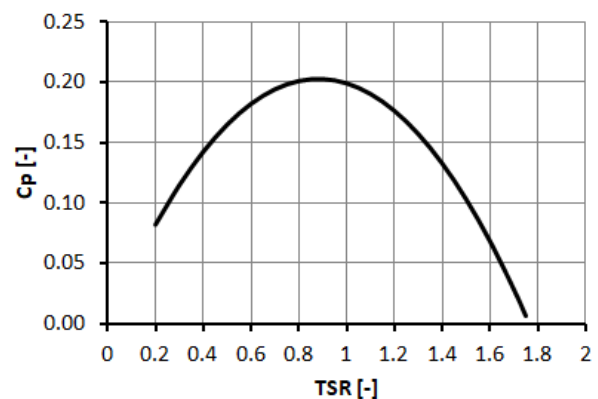


Fig. 11. Typical power characteristics of the Savonius rotor

Measurement of the speed of rotation and wind speed allows calculating the TSR value. It follows from the characteristics in Fig. 11 that knowing the TSR value allows determining the effectiveness of the power generated by the wind turbine. This is an extremely convenient way of judging the quality of the implemented wind turbine controls.

For each wind speed, one can calculate the power for $TSR = 0.9$ at which maximum production of energy could be reached for the Savonius rotor. That allows us to make a plot of the wind turbine power as a function of the rotor rotational speed. Thus, the power characteristics can be presented in terms of the rotor rotational speed in [rpm] in Fig. 12 instead of wind velocity in Fig. 10. In the presented prototype, the rotors have a small diameter, and therefore the rotational speed is quite high.

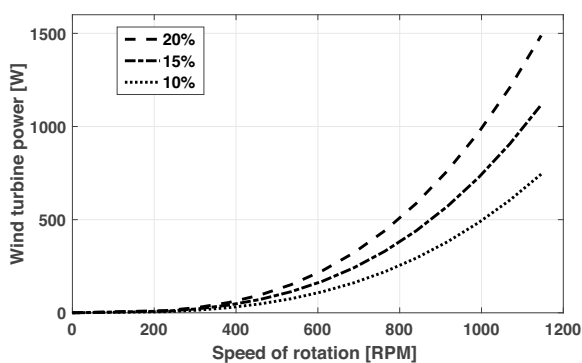


Fig. 12. Wind turbine characteristics in terms of rotor speed for $TSR = 0.9$

Following the numerical results presented in [6, 36], it may be expected that the characteristic of the rotor in an innovative turbine application is generally similar to a single Savonius rotor. However, it can be also expected that due to the small radius of the rotor, the rotational speeds are high, and the nominal power of 800 W (at 20%) is obtained at speeds higher than 900 rpm, as for the small Savonius rotor in Fig. 12. This level of the rotation speed for small diameter rotors in the innovative configuration broadens the general apprehension that Savonius rotors are good for low rotational speeds. The innovative concept of substituting a large Savonius rotor with two small rotors leads to much higher rotational speeds. The increase in rotation is proportional to the ratio of the radius of a large rotor to a small rotor (see Fig. 2).

Traditional small rotational speeds of Savonius wind turbine rotors are a general problem for the choice of power generators. Low velocity of rotation leads to larger and extremely heavy electrical generators. The increased rotation of rotors in the discussed innovative solution introduces an important benefit to the innovative wind turbine. This leads to smaller and much cheaper electrical generators. This is especially important because two generators are needed in the innovative solution, but each for half of the wind turbine power only.

Thanks to the high rotational speed, the prototype of the wind turbine is equipped with core power generators, which are not remarkably effective but can withstand high rotational speeds. 'No-name' scooter motors are easily available in the market and

are used to reduce prototype costs. The tests in a special stand at IMP PAN show that the effectiveness of this motor used as a generator is not high, but it is approximately 70% on average, reaching nearly 80% for nominal conditions. Unfortunately, for small rotational speeds, the effectiveness drops considerably. The nominal speed of rotation for this generator is 1050 rpm, which corresponds to the rotation at a wind speed of 12 m/s and $TSR = 0.9$.

In the presented prototype, the produced power is dissipated into heat to the surrounding air, and it is not connected to any receiver on the ground level. An important feature of the system is that the control algorithm of the power loading of the generators can be modified remotely. The control algorithm is a complex process that determines the quality of the power generation by the wind turbine.

The wind is changing extremely quickly, and there is usually little time to adjust the speed of rotation. Therefore, the rate at which the wind velocity changes should be correlated with the response time of rotors with the variation of loading. This complicated process is still under development. The improvements in this respect are under investigation. The measurements shown in this paper were obtained by a simple algorithm, which increased the load on the rotor when the speed of rotation was increasing, and the rotor was unloaded when the rotational speed was decreasing. This process was implemented with a prescribed gradient of loading and unloading, depending on the speed of rotation. The results presented here directly indicate how the loading process is operating at present.

The measurement system allowed recording the following data:

- Wind velocity V_W [m/s] with 5% error
- Generated voltage U [Volt] with 1% error
- Generated current I [A] with 2% error
- Speed of rotation n [rpm] with 1% error

The sampling frequency was 1 Hz. When adding (or subtracting) independent measurements, the absolute uncertainty of the sum (or difference) is the root sum of squares (RSS) of the individual absolute uncertainties. For the above set of independent variables, the absolute uncertainty is 5.6% [37], which is a high value, but the wind velocity measurement is a decisive factor here.

6. WIND TURBINE EFFECTIVENESS

The generator loading controller is responsible for extracting the maximum power at all wind conditions. It is not known to what extent this objective is fulfilled. This may be judged by the TSR value. TSR is about 0.9 for the Savonius rotor, but in twin rotor configuration is expected to be higher, with $TSR > 1.0$. There are still many options to improve the control algorithm. Wind turbine control is a dynamic process in which the speed of rotation adjustment faces the dynamic variation of the wind speed. This is not a stable process due to the wind unsteadiness. Therefore, the obtained test points form a cloud in the power-wind speed diagram. Figure 13 shows a measurement cloud almost the same for both generators. These diagrams show the limits of experienced wind speed and extracted power.

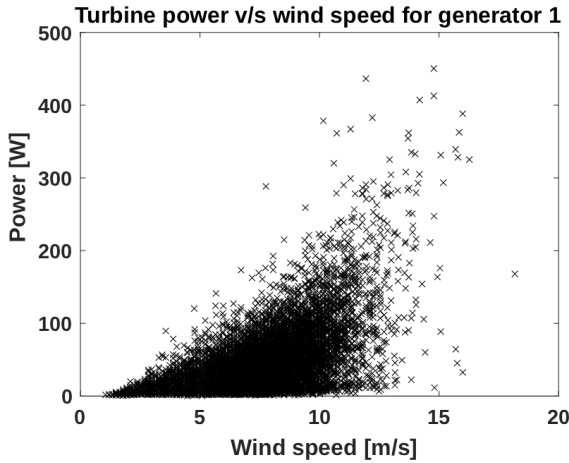


Fig. 13. Measurement points for rotor no. 1

It is difficult to judge the quality of the turbine loading algorithm from these clouds of points. The most effective turbine load controller should lead to $TSR = 0.9$ (for the Savonius rotor) to reach the maximum power at given wind conditions (Fig. 11). As mentioned earlier, one could expect that the maximum power in the innovative wind turbine would occur at even higher TSR values of $1.0 < TSR < 1.2$. Therefore, it is reasonable to look at the obtained wind turbine power in terms of the rotor speed of rotation. The measurements taken deliver rotor speed of rotation [rpm] at each measurement point.

Therefore, it is possible and reasonable to analyze the measurement points in terms of the TSR. As shown in Fig. 7, it happens that rotors stop from time to time, for the tested low wind speed conditions. Such moments influence the test data processing of results. These sample points at which energy is not produced are excluded from the set of data points. The condition to select such points is when the current coming from the generator is equal to zero ($I = 0$), independently of the wind speed.

The TSR values calculated for each measurement point are presented in Fig. 14 with the exclusion of points where no power was produced. Only Rotor-1 is presented because plots for both rotors are remarkably similar.

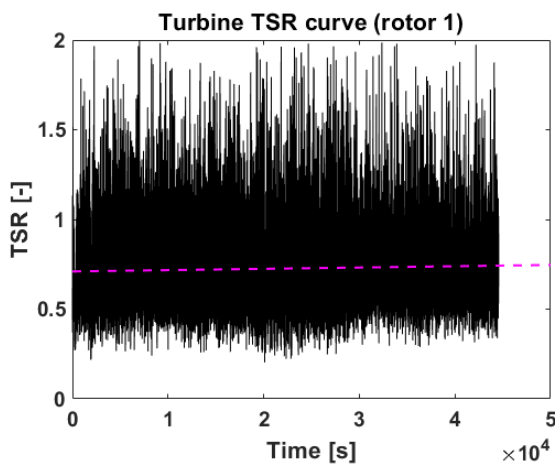


Fig. 14. TSR values for measurement points

Considering the complete set of data points (including $TSR = 0$ cases) that the average of the TSR is 0.68 for Rotor-1 and 0.71 for Rotor-2. Elimination of sample points that do not contribute to energy production does not make a significant difference to the average TSR value but increases the average value. The average TSR for the reduced set of data is 0.72 and 0.75 for Rotor-1 and Rotor-2, respectively (Fig. 14). The observed difference in the TSR value is small. The value of the average TSR is a piece of interesting information because the maximum power for the dual rotor system is expected to be at $TSR > 1.0$, higher than for a single Savonius rotor, as has already been mentioned. This means that the rotors at testing presented here are overloaded, which leads to a reduction in the rotation speed and power.

In Fig. 15, measurement points were organized to show the dependence of generated power as a function of the TSR. The plot shows how the control system works. The increased density of measurement points appears to be around $TSR = 0.9$, but the average value is about 0.75, as mentioned earlier. This is a characteristic feature of the employed load control algorithm. The selection of the test points is not unsatisfactory, because at this TSR, the turbine effectiveness is already sufficient. However, this indicates again that the rotors are overloaded. The maximum density of test points should be located at $TSR > 1.0$, for an appropriate algorithm. Another feature is the TSR value at which the maximum power is attained. One can notice that the points reaching maximum power are obtained at $TSR > 1.0$, which confirms that the power of the wind turbine would be higher with the majority of points for this TSR.

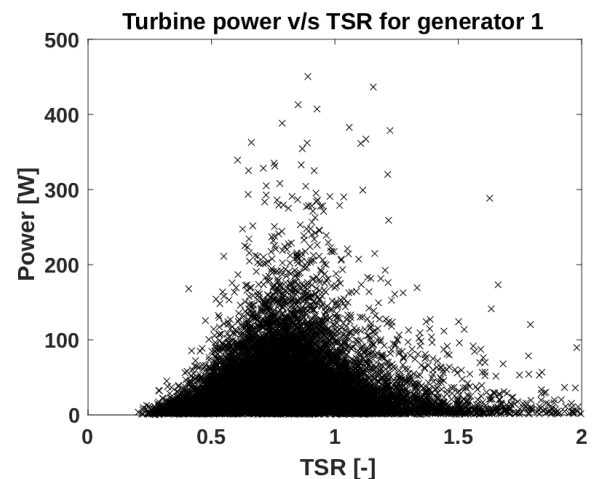


Fig. 15. Generated power as a function of TSR

As shown in Fig. 11, the TSR value is directly connected to the wind turbine effectiveness (C_p). Figure 10 only depicts the results for the Savonius rotor, but with an innovative turbine, the TSR for maximum power should be achieved at $TSR > 1.0$. The measured TSR value for each test point indicates the effectiveness of the wind turbine. Therefore, it is important to color the test points by the corresponding TSR value. The plots, including the TSR value and the effectiveness of characteristics, are presented in Fig. 16.

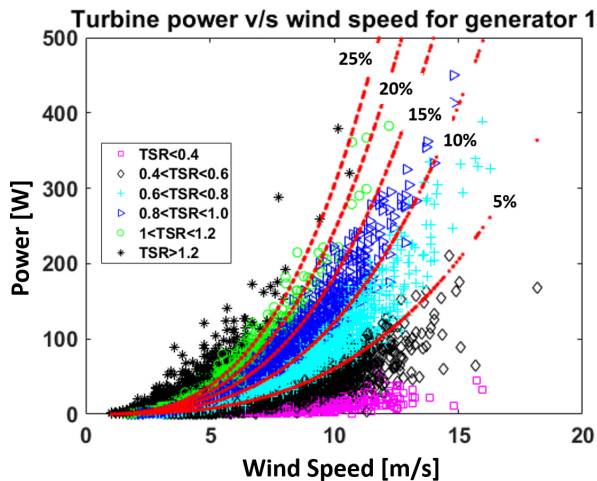


Fig. 16. Test points against effectiveness curves with TSR marked by colors

The measurement points, as in Fig. 13, may be compared against the curve effectiveness in Fig. 16, as shown in Fig. 10. The range of curves for the effectiveness from 5 to 25% includes the main part of the test points. This means that the dynamic processes involved in generator loading algorithms cover a wide spectrum of wind turbine effectiveness cases. There are cases of extremely low effectiveness, but at the same time, a large number of cases prove that the tested wind turbine is remarkably effective.

This indicates a particularly important possibility to improve the load control system to select the points of high effectiveness only. The load control system implemented currently in the wind turbine provides flow cases that are, in a certain sense, random, depending on the dynamic control processes involved. These are the speed of the wind velocity change and the speed of the load adjustment of the system, and also the wind direction change, rotating the whole wind turbine. The relation of these three components makes the tendency of the control system to overload or underload the wind turbine. The mentioned processes depend on the wind speed; therefore, devising the control algorithm is such a demanding task. This has a remarkably considerable influence on the overall effectiveness of the wind turbine and the size of the test points cloud. It is interesting to notice that the indicated ranges of the TSR values, represented with different colors, form wind turbine effectiveness bandwidths. The shape of these bandwidths coincides with the shape of the characteristics of effectiveness.

There are several reasons why the cloud of points is extremely wide. It could be generally expected that when rotors are accelerated from 'zero' to a certain speed, minuscule effectiveness may be recorded because the rotors are still slow when the gust of wind produces a sudden increase in the wind velocity and wind power. In such a case, one obtains low power at a rather low TSR. In another case, the rotors are rotating fast, and the wind suddenly drops. Then, the TSR is high, and the power is high. The above scenario may occur when the rotors respond extremely slowly to the set-up loading. These may be summarized as follows:

Slow rotation and suddenly increased wind speed	Fast rotation and a sudden decrease in wind speed
Low power – high wind	High power – low wind
Low power – low TSR	High power – high TSR

The meaning of the cloud of points depends significantly on the mechanism described. Therefore, it is vital to indicate the TSR value by color for all the points, as shown in Fig. 16. It becomes evident that the results for a particular TSR range are not scattered over the whole measurement domain but form strips in the cloud. In this way, the cloud becomes divided into zones depending on the TSR value. This regular distribution of the TSR over the cloud formed by the measurement points implies that the above mechanism introduces a systematic distribution of the obtained test points.

It becomes evident from the above plots that the increased TSR value of the test points is directly related to the increased effectiveness of the wind turbine. The diagram demonstrates that the maximum effectiveness is obtained for $TSR \geq 1.2$. The plot in Fig. 16 shows that the wind turbine controls should induce conditions of high effectiveness and avoid low effectiveness points. This means that high TSR values are the objective of controls.

7. ENERGY PRODUCTION BY THE TURBINE

Tests of wind turbines in real wind conditions are challenging due to the unsteadiness of wind and the inertness of the turbine rotor operation. It is reported by many authors [13, 15, 30, 38, 39] that wind turbines in real applications are unable to achieve the effectiveness level offered by the manufacturers. Major influence of the wind turbulence on the turbine effectiveness is reported [13, 30]. For lower turbulence levels, the effectiveness of the turbine seems to be closer to the expected turbine performance. As shown in Section 4 of this paper, the presented tests were conducted in a highly turbulent wind, which implies lower energy production than expected.

The energy E (equation (3)) delivered by the wind in time t is

$$E = P \cdot t, \quad (3)$$

where

$$P = E/t = 0.5 \cdot \rho \cdot A \cdot V_W^3. \quad (4)$$

This is the reference energy allowing for the determination of the wind turbine effectiveness, once the energy produced by the generator is measured. In general, the period of the time considered may include cases when energy is not produced by generators when winds are extremely low. The energy delivered by the wind and that produced by the turbine may be determined for each test point. As discussed in previous sections, the considered set of data with 65 646 sample points includes the observation time, including extremely slow winds at which the turbine does not deliver any power. The number of test points producing energy is presented here for each rotor line and is reduced from the above number to 44 577 and 45 553 for Rotor-1 and Rotor-2, respectively. The reduction in the number of test

points means the reduction of measurement time from 18.2 h down to 12.38 h for Rotor-1 and to 12.65 h for Rotor-2. The exclusion of these data points affects the average velocity. Taking the complete set of data points into account, the average wind speed is $V_{AV} = 4.86$ m/s. The exclusion of the unproductive data points mentioned is different for each rotor, and the average velocity of the data set for Rotor-1 and Rotor-2 is $V1_{AV} = 5.57$ m/s and $V2_{AV} = 5.55$ m/s, respectively. The values for both rotors are remarkably similar, and therefore, the effect of the extraction of points is similar for both rotors.

The energy produced by the rotors is determined by the generator output. However, the determination of reference wind energy is not so straightforward. The main question that appears is how much energy included in wind velocity peaks can be utilized by the rotor. The energy production for the set of data in 18.2 hours amounts to 500 Wh, while at the same time, energy produced by the wind reaches 7000 Wh. This means that the wind turbine effectiveness is about 7%. This effectiveness is extremely low but may be considered as acceptable at low wind conditions during the period when the tests were conducted and with extremely high turbulence intensity (TI). It should be also mentioned that the TSR average value is $TSR_{AV} = 0.75$, which means that the extracted power is less than could be expected, in the case of better adjustment of control algorithms leading to higher average TSR values.

A high frequency of wind fluctuations may result in the rotors not being able to follow the wind peaks [7, 13]. The wind fluctuation may result from the unsteadiness of the rotor speed of rotation. Rotors in the innovative wind turbine are exceptionally light with a small moment of inertia due to a small radius and therefore could respond quickly to wind gusts and other wind velocity peaks. The comparison of the wind velocity signal with the rotor 'rpm' allows for drawing some conclusions about the rotor speed response to wind fluctuations.

A careful comparison of wind and rotor signals proves that there is a correlation between wind velocity fluctuations and rotor 'rpm' behavior. However, there is a time shift of approximately 3 seconds in the rotor response. That means that when the wind builds up a velocity peak, the rotor is delayed, missing the chance to absorb the wind energy peak. Figure 17 shows the wind velocity for the selected day (blue line). The red line represents the velocity of the tip of the blade, and V_{TIP} for the selected Rotor-1. The average wind velocity on this day was equal to $V_{AV} = 5.05$ m/s. It is visible in Fig. 17 that the highest tip blade velocity peaks occur a bit later than the corresponding wind velocity peaks. Therefore, it is important to look for a possible correlation between these two signals.

The Pearson correlation coefficient (PCC) was chosen for the presented analysis [40, 41]. It determines the level of the linear dependence between random variables and is expressed by the formula

$$r_{xy} = \frac{\sum_{i=1}^n (x_i - \bar{x})(y_i - \bar{y})}{\sqrt{\sum_{i=1}^n (x_i - \bar{x})^2} \sqrt{\sum_{i=1}^n (y_i - \bar{y})^2}} \quad (5)$$

The vector of variable x represents the wind velocity. The vector of variable y is the velocity of the rotor blade tip, but moving

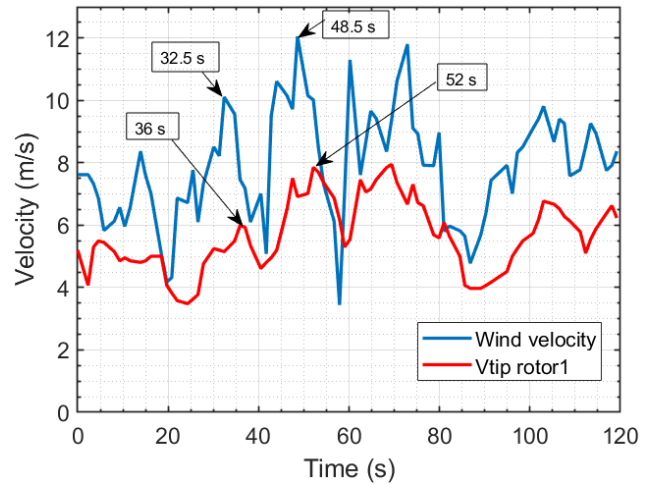


Fig. 17. Relation between wind velocity and Rotor-1 tip velocity

in time, relative to the x vector. In the conducted analysis, the data set for an entire day was considered. The value of the correlation coefficient r_{xy} is in the range $(-1; 1)$. The greater its value, the stronger the linear relationship between the variables. The value of $r_{xy} = 0$ means no linear relationship, and $r_{xy} = 1$ means an exact positive relationship between features; $r_{xy} = -1$ means an exact negative linear relationship. The correlation can be interpreted as strong, weak, or negative [42]. However, such an interpretation is not established, and we cannot take it too strictly. To a good approximation, it can be said that $r_{xy} > 0.5$ represents a strong correlation, and $r_{xy} < 0.5$ means a weak one.

The result is presented in Fig. 18 for Rotor-1 and indicates the highest value of r_{xy} when the time shift between signals is equal to 3.5 sec. It means that we have a strong positive relationship ($r_{xy} = 0.844$) between the wind velocity represented by vector x and the blade tip velocity represented by vector y , but with a time lag of $t_{lag} = 3.5$ sec.

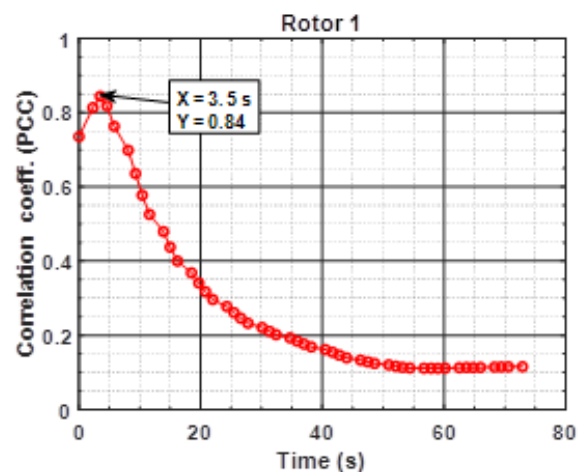


Fig. 18. Correlation of time lag for wind-rotor speed, for both rotors

The plots below indicate that the correlation between wind fluctuations and the rotor behavior exists because the coefficient of correlation $r_{xy} > 0.5$ for an extensive range of time lag. It

is an interesting finding that proves that the rotor inertia does not influence the energy transmission between the wind and the rotor too much.

Rotor-1 displays a maximum correlation for the time lag of 3.5 seconds. The same calculations were made for the Rotor-2, and they also show the correlation coefficient $r_{xy} = 0.84$ and the time lag $t_{lag} = 3.5$ sec because of similarity in behavior with Rotor-1.

If the rotors can use only part of the wind velocity peaks, one can assume that wind fluctuations should be reduced to obtain the effective reference energy delivered by the wind. To illustrate this effect, one can reduce the wind peak height. The reduction of wind peaks by 20% and 50% is shown in the plot in Fig. 19. The included average wind velocity concerns the whole data set, and it does not correspond to the average velocity for the reduced time interval in Fig. 19.

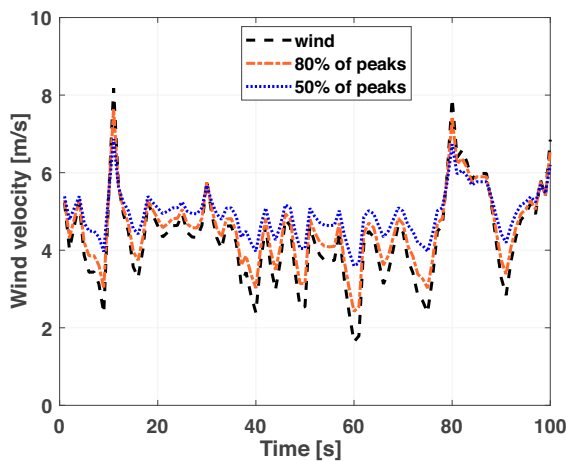


Fig. 19. Reduction of wind speed peaks

Reduction of wind peaks by 20% means reduction of wind energy to 6000 Wh in the test time, which means an increase in wind turbine effectiveness to 8% and when the peaks are reduced by 50% the wind energy drops to about 5200 Wh, and the wind turbine effectiveness will increase to nearly 9%. This effect is consistent with the conclusions of [12] that a reduction in the wind turbulence fluctuations improves the wind turbine effectiveness.

The recorded energy production is the direct outcome of the generators. Therefore, it contains a whole chain of losses involved in the wind turbine operation. The generator effectiveness at these low rotational speeds may be considered even as high as 55%, due to the low quality of the motors used. In addition, the mechanical losses in bearings have some effect, but they are usually exceptionally low and can be neglected here. Therefore, the energy production in the wind turbine system may be estimated at about 55% of what is delivered from the rotor. Considering all these losses, the effectiveness of the rotor itself may be estimated at 17%.

The obtained innovative wind turbine effectiveness is not high, but also the wind conditions of about $V = 5.5$ m/s are not favorable for obtaining higher effectiveness. The used gen-

erator is sensitive to a low speed of rotation, causing a significant reduction in efficiency. It is also apparent that the low value of an average TSR (around 0.7) indicates that there are possibilities to increase the power produced by the wind turbine. There is a necessity to improve the rotor loading, which has to be reduced to allow a higher rotational speed and to obtain higher power.

8. CONCLUSIONS

An innovative twin rotor wind turbine was tested in an urban environment. The wind conditions were incredibly challenging, the average wind speed was incredibly low of about 5.5 m/s. The wind was fluctuating, bearing an exceedingly high turbulence intensity in the order of $TI = 0.4$. These wind conditions did not allow for obtaining high effectiveness of the wind turbine.

The prototype investigated showed that the operation of the innovative turbine corresponded well to the expected performance. The long time of operation revealed excellent endurance of all components of the new wind turbine.

A simple algorithm of rotor loading applied in the prototype facilitated obtaining relatively good turbine performance. However, the obtained average value of TSR around 0.7 indicates that much better energy production could be obtained. The obtained results illustrate that there is a large potential for innovative wind turbine effectiveness improvement. The low value of an average TSR shows that, in general, the rotors are overloaded, reducing the rotational speed considerably. An improved loading algorithm of the rotors should lead to a higher speed of rotation, allowing increased power generation. The objective of the improvements should allow the TSR to increase to about 1.2.

The results obtained have shown that the innovative wind turbine can deliver exquisite performance. However, this calls for further research. The work on the rotor loading algorithm is possible because improved versions can be uploaded remotely. The greatest limitation for the implementation discussed here is access to higher wind conditions.

The presented results will allow for building a prototype with expected effectiveness equal to the Savonius rotor but significantly improved from the point of view of investment costs.

REFERENCES

- [1] A.-S. Yang, Y.-M. Su, C.-Y. Wen, Y.-H. Juan, W.-S. Wang, and C.-H. Cheng, "Estimation of wind power generation in dense urban area," *Appl. Energy*, vol. 171, pp. 213–230, 2016, doi: [10.1016/j.apenergy.2016.03.007](https://doi.org/10.1016/j.apenergy.2016.03.007).
- [2] S. Sachar *et al.*, "Aeroacoustic effect of Savonius rotor segmentation," *Arch. Acoust.*, vol. 50, no. 2, pp. 277–288, 2025, doi: [10.24425/aoa.2025.153665](https://doi.org/10.24425/aoa.2025.153665).
- [3] F. Toja-Silva, O. Lopez-Garcia, C. Peralta, J. Navarro, and I. Cruz, "An empirical-heuristic optimization of the building-roof geometry for urban wind energy exploitation on high-rise buildings," *Appl. Energy*, vol. 164, pp. 769–794, 2016, doi: [10.1016/j.apenergy.2015.11.095](https://doi.org/10.1016/j.apenergy.2015.11.095).
- [4] F.C. Emejeamara and A.S. Tomlin, "A method for estimating the potential power available to building mounted wind turbines

Analysis of a novel vertical axis twin-rotor wind turbine performance in an urban environment

- within turbulent urban air flows,” *Renew. Energy*, vol. 153, pp. 787–800, Jun. 2020, doi: [10.1016/j.renene.2020.01.123](https://doi.org/10.1016/j.renene.2020.01.123).
- [5] A. Lange, M. Pasko, and D. Grabowski, “Selected aspects of wind and photovoltaic power plant operation and their cooperation,” *Bull. Pol. Acad. Sci. Tech. Sci.*, vol. 69, no. 6, p. e139793, 2021, doi: [10.24425/bpasts.2021.139793](https://doi.org/10.24425/bpasts.2021.139793).
- [6] J. Jurasz and J. Mikulik, “Economic and environmental analysis of a hybrid solar, wind and pumped storage hydroelectric energy source: a Polish perspective,” *Bull. Pol. Acad. Sci. Tech. Sci.*, vol. 65, no. 6, pp. 859–869, 2017, doi: [10.1515/bpasts-2017-0093](https://doi.org/10.1515/bpasts-2017-0093).
- [7] P. Doerffer, K. Doerffer, T. Ochrymiuk, and J. Telega, “Variable size twin-rotor wind turbine,” *Energies*, vol. 12, p. 2543, 2019, doi: [10.3390/en12132543](https://doi.org/10.3390/en12132543).
- [8] Y.-H. Juan, A. Rezaeiha, H. Montazeri, B. Blocken, C.-Y. Wen, and A.-S. Yang, “CFD assessment of wind energy potential for generic high-rise buildings in close proximity: Impact of building arrangement and height,” *Appl. Energy*, vol. 321, p. 119328, 2022, doi: [10.1016/j.apenergy.2022.119328](https://doi.org/10.1016/j.apenergy.2022.119328).
- [9] D. Saeidi, A. Sedaghat, P. Alamdari, and A.A. Alemrajabi, “Aerodynamic design and economical evaluation of site specific small vertical axis wind turbines,” *Appl. Energy*, vol. 101, pp. 765–775, 2013.
- [10] S. Roy and U.K. Saha, “Wind tunnel experiments of a newly developed two-bladed Savonius-style wind turbine,” *Appl. Energy*, vol. 137, pp. 117–125, 2015, doi: [10.1016/j.apenergy.2014.10.022](https://doi.org/10.1016/j.apenergy.2014.10.022).
- [11] L.A. Danao, J. Edwards, O. Eboibi, and R. Howell, “A numerical investigation into the influence of unsteady wind on the performance and aerodynamics of a vertical axis wind turbine,” *Appl. Energy*, vol. 116, no. 1, pp. 111–124, 2014.
- [12] D. Schulz, “Improved grid integration of wind energy systems,” *Bull. Pol. Acad. Sci. Tech. Sci.*, vol. 57, no. 4, 2009, doi: [10.2478/v10175-010-0133-0](https://doi.org/10.2478/v10175-010-0133-0).
- [13] L.C. Pagnini, M. Burlando, and M.P. Repetto, “Experimental power curve of small-size wind turbines in turbulent urban environment,” *Appl. Energy*, vol. 154, pp. 112–121, 2015, doi: [10.1016/j.apenergy.2015.04.117](https://doi.org/10.1016/j.apenergy.2015.04.117).
- [14] M.M.A. Bhutta, N. Hayat, A.U. Farooq, Z. Ali, S.R. Jamil, and Z. Hussain, “Vertical axis wind turbine – a review of various configurations and design techniques,” *Renew. Sustain. Energy Rev.*, vol. 16, pp. 1926–1939, 2012.
- [15] A.S. Saad, I.I. El-Sharkawy, S. Ookawara, and M. Ahmed, “Performance enhancement of twisted-bladed Savonius vertical axis wind turbines,” *Energy Convers. Manage.*, vol. 209, p. 112673, 2020.
- [16] R. Jia, H. Xia, S. Zhang, W. Su, and S. Xu, “Optimal design of Savonius wind turbine blade based on support vector regression surrogate model and modified flower pollination algorithm,” *Energy Convers. Manage.*, vol. 270, p. 116247, 2022, doi: [10.1016/j.enconman.2022.116247](https://doi.org/10.1016/j.enconman.2022.116247).
- [17] W. Tian, Z. Mao, B. Zhang, and Y. Li, “Shape optimization of a Savonius wind rotor with different convex and concave sides,” *Renew. Energy*, vol. 117, pp. 287–299, Mar. 2018, doi: [10.1016/j.renene.2017.10.067](https://doi.org/10.1016/j.renene.2017.10.067).
- [18] N. Aloma and U.K. Saha, “Influence of blade profiles on Savonius rotor performance: Numerical simulation and experimental validation,” *Energy Convers. Manage.*, vol. 186, pp. 267–277, 2019, doi: [10.1016/j.enconman.2019.02.058](https://doi.org/10.1016/j.enconman.2019.02.058).
- [19] S. Roy and A. Ducoin, “Unsteady analysis on the instantaneous forces and moment arms acting on a novel Savonius-style wind turbine,” *Energy Convers. Manage.*, vol. 121, pp. 281–296, 2016, doi: [10.1016/j.enconman.2016.05.044](https://doi.org/10.1016/j.enconman.2016.05.044).
- [20] P. Strojny, “Study on the efficiency of small-scale wind turbine with rotor adapted for low wind speeds,” *Bull. Pol. Acad. Sci. Tech. Sci.*, vol. 72, no. 6, p. e151954, 2024, doi: [10.24425/bpasts.2024.151954](https://doi.org/10.24425/bpasts.2024.151954).
- [21] L.B. Kothe, S.V. Möller, and A.P. Petry, “Numerical and experimental study of a helical Savonius wind turbine and a comparison with a two-stage Savonius turbine,” *Renew. Energy*, vol. 148, pp. 627–638, Apr. 2020, doi: [10.1016/j.renene.2019.10.151](https://doi.org/10.1016/j.renene.2019.10.151).
- [22] S. Torres, A. Marulanda, M.F. Montoya, and C. Hernandez, “Geometric design optimization of a Savonius wind turbine,” *Energy Convers. Manage.*, vol. 262, p. 115679, 2022, doi: [10.1016/j.enconman.2022.115679](https://doi.org/10.1016/j.enconman.2022.115679).
- [23] K. Doerffer, J. Telega, P. Doerffer, P. Hercel, and A. Tomporowski, “Dependence of power characteristics on Savonius rotor segmentation,” *Energies*, vol. 14, p. 2912, 2021, doi: [10.3390/en14102912](https://doi.org/10.3390/en14102912).
- [24] U.K. Saha, S. Thotla, and D. Maity, “Optimum design configuration of Savonius rotor through wind tunnel experiments,” *J. Wind Eng. Ind. Aerodyn.*, vol. 96, pp. 1359–1375, 2008.
- [25] C. Jian, J. Kumbernuss, L. Zhang, L. Lin, and H. Yang, “Influence of phase-shift and overlap ratio on Savonius wind turbine’s performance,” *J. Sol. Energy Eng.*, vol. 134, p. 011016, 2012.
- [26] T. Hayashi, Y. Li, Y. Hara, and K. Suzuki, “Wind tunnel tests on a three-stage out-phase Savonius rotor,” *JSME Int. J. Ser. B*, vol. 48, p. 2005, 2004.
- [27] P. Jaohindy, S. McTavish, F. Garde, and A. Bastide, “An analysis of the transient forces acting on Savonius rotors with different aspect ratios,” *Renew. Energy*, vol. 55, pp. 286–295, 2013.
- [28] K. Sobczak, “Numerical investigations of an influence of the aspect ratio on the Savonius rotor performance,” in *Proc. XXIII Fluid Mech. Conf. (KKMP 2018)*, Zawiercie, Poland, 2018, *J. Phys. Conf. Ser.*, vol. 1101, p. 012034.
- [29] S. Roy and A. Ducoin, “Unsteady analysis on the instantaneous forces and moment arms acting on a novel Savonius-style wind turbine,” *Energy Convers. Manage.*, vol. 121, pp. 281–296, 2016.
- [30] L. Pagnini, G. Piccardo, and M.P. Repetto, “Full scale behaviour of a small size vertical axis wind turbine,” *Renew. Energy*, vol. 127, pp. 41–55, 2018, doi: [10.1016/j.renene.2018.04.032](https://doi.org/10.1016/j.renene.2018.04.032).
- [31] A.H. Shaban, A.K. Resen, and N. Bassil, “Weibull parameters evaluation by different methods for windmills farms,” *Energy Rep.*, vol. 6, suppl. 3, pp. 188–199, 2020.
- [32] Q. Li, J. Wang, and H. Zhang, “Comparison of the goodness-of-fit of intelligent-optimized wind speed distributions and calculation in high-altitude wind-energy potential assessment,” *Energy Convers. Manage.*, vol. 247, p. 114737, 2021.
- [33] S. Sachar, S. Shubham, P. Doerffer, A. Ianakiev, and P. Flaszynski, “Wind speed probabilistic forecast based wind turbine selection and siting for urban environment,” *IET Renewable Power Gener.*, vol. 18, no. 15, pp. 3285–3300, 2024, doi: [10.1049/rpg2.13132](https://doi.org/10.1049/rpg2.13132).
- [34] M. McHugh, “The Chi-square test of independence,” *Biochem. Med.* vol. 23, no. 2, pp. 143–149, 2013, doi: [10.11613/BM.2013.018](https://doi.org/10.11613/BM.2013.018).

S. Sachar, P. Doerffer, P. Flaszynski, K. Doerffer, J. Grzelak, and A. Reiter

- [35] A.K. Azad, M.G. Rasul, and T.F. Yusaf, "Statistical diagnosis of the best Weibull methods for wind power assessment for agricultural application," *Energies*, vol. 7, pp. 3056–3085, 2014, doi: [10.3390/en7053056](https://doi.org/10.3390/en7053056).
- [36] A. Chiappalone, "Studio di Una Turbina Eolica Innovativa ad Asse Verticale", M.Sc. thesis, Scuola Politecnica, Univ. Genova, 2016.
- [37] S.G. Rabinovich, *Measurement Errors and Uncertainties: Theory and Practice*, USA: Springer New York, 2005.
- [38] S.A. Rolland, W. Newton, A.J. Williams, T.N. Croft, and D.T. Gethin, "Simulation technique for the design of a vertical axis wind turbine device with experimental validation," *Appl. Energy*, vol. 111, pp. 1195–1203, 2013.
- [39] S.A. Rolland *et al.*, "Benchmark experiments for simulations of a vertical axis wind turbine," *Appl. Energy*, vol. 111, pp. 1183–1194, 2013.
- [40] Penn State University, Eberly College of Science, "2.6 – (Pearson) Correlation Coefficient r ," *STAT 462*. [Online]. Available: <https://online.stat.psu.edu/stat462/node/96> [Accessed: 10 Jul. 2021].
- [41] H.E. Soper, A.W. Young, B.M. Cave, A. Lee, and K. Pearson, "On the distribution of the correlation coefficient in small samples," *Biometrika*, vol. 11, no. 4, pp. 328–413, 1917, doi: [10.1093/biomet/11.4.328](https://doi.org/10.1093/biomet/11.4.328).
- [42] J. Cohen, *Statistical Power Analysis for the Behavioral Sciences*, 2nd ed. New York: Routledge, 1988, doi: [10.4324/9780203771587](https://doi.org/10.4324/9780203771587).